

Effect of Differential Tracer Washout During SPECT Acquisition

Jonathan M. Links, Terry L. Frank, and Lewis C. Becker

Divisions of Nuclear Medicine and Cardiology, The Johns Hopkins Medical Institutions, Baltimore, Maryland

A central assumption in SPECT is that the projection data are "consistent," that is, the camera views an unchanging distribution during acquisition. Several new radiotracers of interest, including ^{99m}Tc -teboroxime (Cardiotec[®]), have rapid clearance from the myocardium. Furthermore, the washout is different in normal and ischemic tissues. We used computer simulations to estimate the effect of this differential washout on quantification of the severity of ischemia. We simulated defect-to-normal myocardial activity ratios of 1 (no defect), 0.8, 0.6, 0.4, 0.2, and 0 (complete defect), with single defects placed either in the lateral wall or apex, and SPECT acquisitions of 1, 3, 6, 12, and 24 total minutes. We modeled washout with a monoexponential curve whose clearance half-time was 5.9 min for "normal myocardium" and 9.3 min for "ischemic myocardium." We found that differential washout from normal and ischemic zones produced image artifacts and errors in defect quantification for acquisitions longer than 3 min. With longer acquisitions, the degree of ischemia was significantly underestimated, with increasing error at longer acquisition times. In addition, in the "no defect" situation an apparent small lateral wall defect (relative to the apex) was present. Finally, lateral wall defects produced artifacts (streaks and reduced apparent activity) in the opposite (medial) wall. Differential normal/ischemic zone washout during SPECT acquisition produces artifacts and errors in quantification, whose severity is dependent on acquisition length, actual defect severity, and defect location.

J Nucl Med 1991; 32:2253-2257

A central assumption in any image reconstruction approach is that the projection data are "consistent;" that is, all projection data come from the same "object." In SPECT, the object is the distribution of radioactivity within the subject being scanned; this distribution must remain unchanged during the entire acquisition process. In practice, this typically requires a fairly stationary distribution for 20-30 min. In 1983, Ip tried to analytically estimate the artifacts that would result from a change in distribution with time (*1*). In 1987, Bok reported on the

results of computer simulations and phantom experiments of a changing distribution (*2*). In both of these studies, the change in distribution was modeled as a scalar change which equally effected all values within a given projection.

Much interest has been paid to new radiotracers of myocardial perfusion, with particular focus on SPECT. One of these tracers, ^{99m}Tc -teboroxime (Cardiotec[®]), is known to have fairly rapid washout from both normal and ischemic myocardium. While this characteristic may be useful in permitting serial studies in a single session, it could produce artifacts in SPECT reconstructions. Furthermore, since the washout from normal and ischemic myocardium is different ("differential washout"), the studies above do not indicate the degree of artifact which might be produced. We therefore performed a series of computer simulations which more accurately represented this situation, to assess the effects of this so-called differential washout during SPECT acquisition on quantification of the degree of ischemia.

METHODS

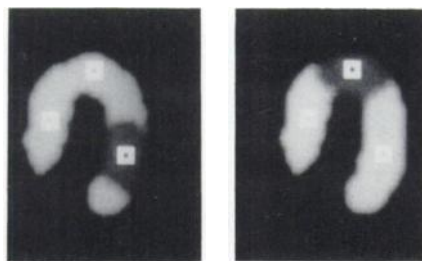
We manually generated a stylized horseshoe-shaped "transaxial left ventricular" slice within a 64×64 matrix. We used a mid-heart transaxial slice from a normal volunteer as a template to accurately generate a horseshoe of realistic size and shape. All pixels within this horseshoe were given the same value; pixels outside the horseshoe were set to zero. Multiple copies of this image were generated. We then generated a "defect zone" on either the "lateral wall" or at the "apex." This zone occupied approximately 25% of the horseshoe. All pixels within the defect zone were given a uniform value, equivalent to either 0, 20, 40, 60, 80, or 100% of the pixel value in the rest of the horseshoe. Each test image thus contained two zones within the horseshoe: a large "normal" zone and a smaller "ischemic" zone, with a simulated defect-to-normal ratio of either 1 (no defect), 0.8, 0.6, 0.4, 0.2, or 0 (complete defect).

Simulated projection data sets were obtained by reprojection along parallel rays through the test images described above. To produce a given projection's data, pixel values were summed, with no simulation of attenuation effects or noise. In practice, a single horizontal reprojection routine was implemented, and the test (transaxial slice) image rotated between reprojection angles with an array processor routine provided by the manufacturer (Technicare).

Differential washout was modeled as monoexponential tracer clearance from the "normal" and "ischemic" zones. We used a

Received Jan. 14, 1991; revision accepted Aug. 13, 1991.
For reprints contact: Jonathan M. Links, PhD, Nuclear Medicine, Johns Hopkins Medical Institutions, 615 North Wolfe St., Baltimore, MD 21205-2179.

FIGURE 1. Simulated original transaxial left ventricular slice. Left: Lateral wall defect. Right: Apical defect. Defect-to-normal ratio = 0.40. Both slices show same three ROIs used for analysis.



washout half-time of 5.9 min for normal “myocardium,” and 9.3 min for ischemic “myocardium,” as experimentally determined by Stewart and coworkers in dogs (3). At each reprojection angle, we reduced the pixel values in the test image, separately in the normal and ischemic zones, by the appropriate factors, prior to reprojection at that angle. We simulated total acquisition times of 1, 3, 6, 12, and 24 min. Thirty equi-angular projections over 180° were obtained; these were then used in a standard filtered backprojection reconstruction algorithm (with a ramp filter) provided by the manufacturer to produce a “transaxial left ventricular slice.”

Quantitative accuracy of the reconstructed slice was assessed by placing square regions of interest in the center of the “ischemic” zone and in representative “normal” zones, and comparing observed with true defect-to-normal zone ratios (Fig. 1). For those simulations with the lateral wall defect, the apex was used as the normal reference zone, because the medial wall opposite the defect contained reconstruction artifacts (see below). For those simulations with the apical defect, the average of the observed apical defect-to-lateral wall and apical defect-to-medial wall ratios was used.

RESULTS

We first validated our simulation approach by reconstructing a simulated point source positioned at various locations; in the absence of washout this point was perfectly reconstructed. We then used the lateral wall defect case, without washout, to test the accuracy of the reconstruction implementation. No artifacts were visually observed in any of the images. The quantitative results shown in Table 1 indicate negligible reconstruction errors in the absence of washout.

TABLE 1
Lateral Wall Defect (No Washout)

Actual Defect/ Normal Ratio*	Observed Defect/ Normal Ratio†	%Error‡
1.0	0.99	-1.00
0.8	0.79	-1.25
0.6	0.60	0
0.4	0.40	0
0.2	0.19	-5.00
0.0	0.01	—

* Actual lateral wall defect-to-normal.

† Observed lateral wall defect-to-normal apex ratio.

‡ (Observed-actual)/actual defect-to-normal ratio.

A total of 60 reconstructed images were produced with washout, representing defect-to-normal ratios of 1 (no defect), 0.8, 0.6, 0.4, 0.2, and 0 (complete defect), with total acquisition times of 1, 3, 6, 12, and 24 min, for both lateral wall and apical defects. For acquisition times longer than 3 min, the images with the lateral wall defect showed striking artifacts in the medial wall opposite the defect. These artifacts took the form of bands of decreased “activity,” which appeared to emanate from the defect zone, along with small streaks of increased activity outside the actual myocardial border (Fig. 2). The severity of these artifacts increased with increasing total acquisition time. The images with the apical defect showed similar streaking outside the myocardial border (Fig. 2).

Quantitative results are presented in Table 2 and Figure 3 for the lateral wall defect and Table 3 and Figure 4 for the apical defect. Because of the artifacts noted above, we used the apex as the normal reference zone for the lateral wall defect and the average of the medial and lateral walls as the reference for the apical defect. For the lateral wall defect, there was progressive underestimation of the severity of the defect with increasing total acquisition time. The greatest errors were observed for the largest defects (i.e., 0.2 defect-to-normal ratio). There was also an apparent “defect” in the medial wall at longer acquisition times. For the apical defect, there was also progressive underestimation of the severity of the defect with increasing total acquisition time for mild to moderate defects (i.e., 0.8, 0.6, 0.4 defect-to-normal ratios), but an overestimation of severity for the most severe case (0.2 defect-to-normal ratio). There was again an apparent “defect” in the medial wall relative to the lateral wall at longer acquisition times.



FIGURE 2. Reconstructed transaxial slices from simulated acquisition times ranging from 1 to 24 min. Left column: Apical defect. Right column: Lateral wall defect. Original slice has defect-to-normal ratio = 0.40.

TABLE 2
Lateral Wall Defect (With Washout)

Actual Defect/ Normal Ratio*	Observed Defect/ Normal Ratio†	Medial Wall/ Apex Ratio‡	%Error§
Total Acquisition Time = 1 min			
1.0	0.98	0.97	- 1.94
0.8	0.80	0.97	0.41
0.6	0.60	0.97	0.61
0.4	0.40	0.96	0.44
0.2	0.21	0.96	4.02
0.0	0.01	0.96	—
Total Acquisition Time = 3 min			
1.0	0.98	0.95	-2.23
0.8	0.84	0.94	4.62
0.6	0.63	0.94	5.29
0.4	0.42	0.93	5.55
0.2	0.22	0.93	7.62
0.0	0.01	0.92	—
Total Acquisition Time = 6 min			
1.0	0.97	0.91	-3.12
0.8	0.88	0.90	10.17
0.6	0.66	0.89	10.47
0.4	0.45	0.88	12.62
0.2	0.23	0.87	16.53
0.0	0.02	0.86	—
Total Acquisition Time = 12 min			
1.0	0.95	0.85	-5.05
0.8	0.94	0.80	17.93
0.6	0.71	0.79	19.15
0.4	0.49	0.77	21.99
0.2	0.26	0.75	30.77
0.0	0.03	0.74	—
Total Acquisition Time = 24 min			
1.0	0.84	0.70	-16.47
0.8	0.96	0.63	20.59
0.6	0.74	0.60	23.61
0.4	0.49	0.55	22.88
0.2	0.26	0.52	28.08
0.0	0.02	0.48	—

* Actual lateral wall defect-to-normal ratio.

† Observed lateral wall defect-to-normal apex ratio.

‡ Observed opposite medial wall-to-apex ratio.

§ (Observed-actual)/actual defect-to-normal ratio.

DISCUSSION

SPECT reconstruction is based on a fundamental assumption that the projection data are "consistent." This consistency implies that each projection views the entire object, and that the radioactivity distribution does not change between projections. Such is not the case for radiotracers that have rapid washout from the organ of interest, such as ^{99m}Tc-teboroxime in the myocardium.

In 1987, Bok and coworkers presented results of computer simulation which seemed to indicate that as long as the tracer concentration changed by less than a factor of two during the SPECT acquisition, artifacts (which they called "image distortion") were not visible, although measurements of spatial resolution showed some changes (2). These results have been used by others to justify the use of radiotracers such as teboroxime with SPECT. Even so, when emphasis is placed on quantification of abnormal

zones within an image, the results of Bok may not apply, particularly in the setting of differential washout rates in normal and diseased zones. We in fact found that this differential washout, which was not part of Bok's computer simulations, does affect both image quality and quantification.

Our simulations were based on observed washout rates in dogs and the assumption of monoexponential washout. Stewart and coworkers have subsequently reported that teboroxime washout is not monoexponential, but rather is biexponential; 67% of the activity clears with a half-time of 2.3 min, while the residual activity clears with a much longer half-time, 20 min, under resting flow conditions (4). Unfortunately, Stewart did not report separate half-time values for normal and ischemic zones. Based on his earlier work, and our own observations, we believe that differential washout exists, and chose to model the effects

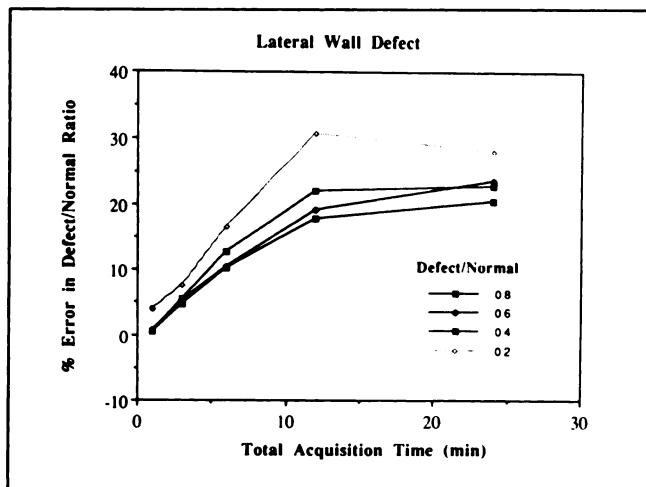


FIGURE 3. Error in defect-to-normal quantification as a function of acquisition time for the lateral wall defect simulation. Apex was used as normal reference zone.

of this nonuniform washout. For the case of *uniform* washout, whether mono- or bi-exponential, the results of Bok apply.

The difference in results between lateral wall and apical defects is most likely due to differences in the contribution of both the defect zone activity to normal areas and the contribution of normal zone activity to the defect during the backprojection process. In the case of the lateral wall defect, the reduced activity from this wall, and the normal activity in the medial wall, would influence each other during the backprojection process over a wide range of projection angles, leading to a reduction in medial wall counts and an increase in lateral wall activity in the reconstruction. Indeed, for long acquisition times the artifactual medial wall "defect" was of greater severity than the actual lateral wall defect for the mildest defect. In the case of the apical defect, the relative "isolation" of this

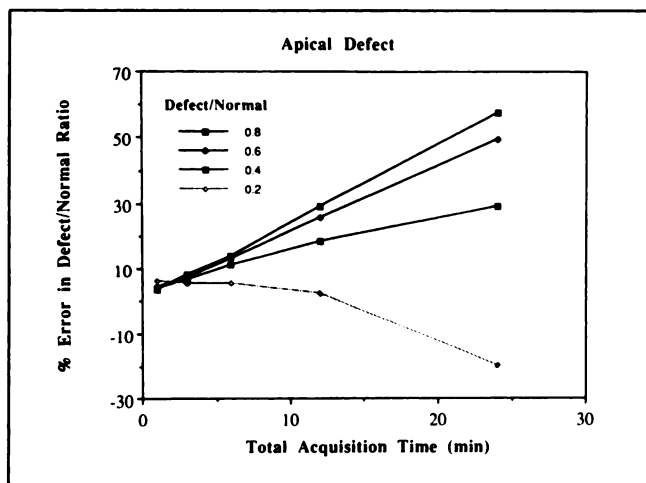


FIGURE 4. Error in defect-to-normal quantification as a function of acquisition time for the apical defect simulation. Average of medial and lateral walls was used as normal reference.

TABLE 3
Apical Defect (With Washout)

Actual Defect/ Normal Ratio*	Observed			%Error [†]
	Medial Wall/Lateral Wall Ratio [†]	Observed Apex/Lateral Wall Ratio [‡]	Observed Apex/Medial Wall Ratio [§]	
Total Acquisition Time = 1 min				
1.0	0.99	1.02	1.03	2.60
0.8	0.99	0.82	0.83	3.64
0.6	0.99	0.62	0.63	4.37
0.4	0.98	0.41	0.42	3.99
0.2	0.99	0.21	0.21	6.45
0.0	0.98	0.01	0.01	—
Total Acquisition Time = 3 min				
1.0	0.97	1.02	1.05	3.66
0.8	0.97	0.85	0.88	8.13
0.6	0.97	0.64	0.65	7.57
0.4	0.98	0.42	0.43	6.48
0.2	0.98	0.21	0.21	5.41
0.0	0.98	0.00	0.00	—
Total Acquisition Time = 6 min				
1.0	0.94	1.03	1.09	6.28
0.8	0.96	0.89	0.93	13.79
0.6	0.96	0.66	0.69	13.00
0.4	0.96	0.44	0.45	11.34
0.2	0.96	0.21	0.22	5.49
0.0	0.97	0.00	0.00	—
Total Acquisition Time = 12 min				
1.0	0.90	1.07	1.19	12.73
0.8	0.92	0.99	1.08	29.10
0.6	0.93	0.73	0.78	25.88
0.4	0.93	0.46	0.49	18.56
0.2	0.94	0.20	0.21	2.43
0.0	0.95	0.00	0.00	—
Total Acquisition Time = 24 min				
1.0	0.84	1.20	1.43	31.52
0.8	0.84	1.15	1.37	57.38
0.6	0.85	0.83	0.97	49.27
0.4	0.88	0.49	0.55	29.25
0.2	0.90	0.15	0.17	-19.66
0.0	0.92	0.00	0.00	—

* Actual apical defect-to-normal ratio.

† Observed "normal" medial-to-"normal" lateral wall ratio.

‡ Observed apical defect-to-lateral wall ratio.

§ Observed apical defect-to-medial wall ratio.

† (Observed-actual)/actual apical defect-to-normal ratio (observed ratio = average of apical-to-lateral and apical-to-medial ratio).

area of the myocardium, coupled with slower clearance, apparently led to an increase in reconstructed apical activity which was most severe when the actual apical activity was closest to normal. Indeed, when the apical activity was decreased to a low value (i.e., 0.2 of normal), there was an underestimation relative to the normal zone.

We specifically chose not to incorporate the effects of attenuation, depth-dependent spatial resolution changes, or noise into our simulations in order to isolate washout artifacts. In our study, the direction of rotation (clockwise versus counterclockwise) was irrelevant; reprojection in either direction yielded the same simulated projection data. In real world imaging, with attenuation and resolution effects, rotation direction would affect the influence

of differential washout on artifacts, as those areas of the myocardium closest to the camera in a given view would dominate that projection's data. Thus, if a "defect" was closest to the camera in initial views, differential washout would be less of a problem than if the defect was closest in the final views, when the *change* from the initial distribution was greatest. For example, over a 12-min imaging period the activity in a normal zone and a zone with a 40% initial reduction equalize.

In practice, we recommend that the total acquisition time for a single 180° or 360° rotation not exceed 5 min for optimum teboroxime imaging. It may be preferable, in fact, to sequentially acquire multiple short (e.g., 1–3 min) acquisitions and add the data together afterwards. Because backprojection is a linear process, either projection data or reconstructed images could be summed. This approach would produce images from more consistent projection data, eliminating the artifacts observed here. It should be noted, however, that the differential washout from normal and ischemic zones would still produce an underestima-

tion of ischemia in these images, as the resulting images would represent the *average* activity in the normal and ischemic zones during the total acquisition period over which the data were summed.

ACKNOWLEDGMENT

Supported in part by USPHS grants HL17655 (Specialized Center of Research in Ischemic Heart Disease) and CA32845.

REFERENCES

1. Ip WR, Holden JE, Winkler SS. A study of the image discrepancies due to object time dependence in transmission and emission tomography. *Phys Med Biol* 1983;28:952–953.
2. Bok BD, Bice AN, Clausen M, Wong DF, Wagner HN. Artifacts in camera based single photon emission tomography due to time activity variation. *Eur J Nucl Med* 1987;13:439–442.
3. Stewart RE, Heyl B, Blumhardt R, et al. Differential post-stenotic myocardial SQ30217 kinetics following adenosine and dipyridamole-induced hyperemic stress [Abstract]. *J Nucl Med* 1990;31:785.
4. Stewart RE, Schwaiger M, Hutchins GD, et al. Myocardial clearance kinetics of technetium-99m-SQ30217: a marker of regional myocardial blood flow. *J Nucl Med* 1990;31:1183–1190.